

## Sideband cooling of ions in radio-frequency traps

E. Peik, J. Abel, Th. Becker, J. von Zanthier, and H. Walther

*Max-Planck-Institut für Quantenoptik and Sektion Physik der Ludwig-Maximilians-Universität München, Hans-Kopfermann-Strasse 1, 85748 Garching, Germany*

(Received 25 February 1999)

An experimental study of sideband laser cooling of trapped ions in miniature radio-frequency traps is presented.  $\text{In}^+$  ions are laser cooled by exciting the narrow intercombination line  $5s^2\ ^1S_0 \rightarrow 5s5p\ ^3P_1$ , which shows resolved sidebands due to the vibrational motion of the ions in the trap. The influence of the micromotion at the frequency of the oscillating trapping field is investigated. Heating processes through coupling with the trapping field occur for certain regions of negative laser detuning. A method of bichromatic sideband cooling is introduced that combines efficient cooling from high temperatures with the possibility of reaching low mean vibrational quantum numbers  $\langle n \rangle < 1$  by using narrow optical transitions. This technique allows recording of high-resolution excitation spectra of the cooling transition in the Lamb-Dicke regime and thus determination of  $\langle n \rangle$ . Single ions as well as two-ion Coulomb crystals have been cooled to temperatures below  $100\ \mu\text{K}$ , and population of the ground state of motion to more than 50% over long time scales is demonstrated. These values are close to the lower limit for the detection of vibrational excitation with the present method. [S1050-2947(99)08407-3]

PACS number(s): 32.80.Lg, 42.50.Vk

### I. INTRODUCTION

Of the various proposed and realized methods for laser cooling of atoms or trapped ions sideband cooling [1] is conceptually the simplest and most efficient: It allows a trapped particle to be cooled to the quantum-mechanical ground state of a harmonic trap potential. The process can be regarded as anti-Stokes Raman scattering of the pseudomolecule formed by the atom and the trap [2]. If the linewidth of an optical transition in this atom is smaller than the vibrational frequency in the trap, both electronic levels of the transition split into a ladder of resolved vibrational levels. The absorption spectrum consists of a carrier at the resonance of the free atom and sidebands at multiples of the vibrational frequency. With a laser tuned to the  $m$ th lower-frequency sideband, each absorption of a photon will reduce the vibrational energy of the atom by  $m$  quanta. Since the subsequent spontaneous reemission will on the average not change the vibrational excitation, repeated photon scattering leads to efficient cooling of the atom. This cooling will continue until the absorption probability for the low-frequency sidebands decreases with the approach of the ground state of the trap. The final temperature is limited by heating through the photon recoil.

Despite these obvious advantages of sideband cooling, relatively few experiments have made use of this method so far. This is because the regime where the oscillation frequency  $\omega$  is bigger than the natural linewidth  $\Gamma$  of an optical transition (the so-called "strong binding regime") is not easily accessible. Vibrational frequencies of ions in standard electromagnetic traps are of the order of 1 MHz, whereas linewidths of electric dipole transitions in positive ions are in the range 20–50 MHz. In this "weak binding regime" with  $\Gamma > \omega$  laser cooling of trapped ions is analogous to Doppler cooling of free atoms [3]. The minimum temperature is given by the Doppler limit  $k_B T = \hbar \Gamma / 2$  [2], and the mean vibrational quantum number is  $\langle n \rangle = \Gamma / 2\omega > 1$ . The first experi-

ments with cooling on resolved sidebands therefore used a strongly forbidden optical transition [4] or stimulated Raman transitions [5]. In these cases, however, sideband cooling is inevitably slow and was used only to extract a few vibrational quanta from Doppler-precooled ions. In both experiments the vibrational ground state was reached to a very good approximation (mean quantum number  $\langle n \rangle \approx 0.05$ ). Raman sideband cooling was also recently applied to neutral atoms in optical traps [6,7]. In the present paper we describe experiments with trapped  $\text{In}^+$  ions that open a new regime of parameters, since here cooling is performed on an intercombination line  $5s^2\ ^1S_0 \rightarrow 5s5p\ ^3P_1$  with a natural linewidth  $\Gamma/2\pi$  of 360 kHz [8]. This makes it easy to reach the strong binding regime and also ensures fast and efficient cooling, so that other methods of precooled are not required. Only one cooling method is used to reduce the vibrational excitation of the ion from an initial  $\langle n \rangle \approx 10^8$  close to  $\langle n \rangle = 0$ . We report experiments with single ions as well as with two ions, forming a Coulomb crystal.

Laser cooling of trapped ions was motivated by the possible application in an optical frequency standard [9] where the relativistic Doppler shift as well as the Stark shift due to the trap potential are reduced at low temperatures. Cooling to the ground state also affords possibilities of studying a well-controlled mechanical quantum oscillator experimentally. This led to production of nonclassical states of motion [10], investigation of quantum decoherence phenomena [11], a proposal to use trapped ions as the register of a quantum computer [12], and realization of a quantum logic gate [13].

### II. THEORY

Most theoretical treatments of sideband cooling consider a static harmonic trap [2,14], neglecting the time dependence of the potential in radio-frequency ion traps. In this model a running laser wave  $\propto \exp(ikr)$  of wave number  $k$  induces transitions between the eigenstates  $|n\rangle$  and  $|n'\rangle$  of a har-

monic oscillator. The relevant transition matrix elements are [2]

$$U_{n',n} = \langle n' | \exp(ikr) | n \rangle \quad (1)$$

$$= \exp(-\eta^2/2) \sqrt{\frac{n_{<}!}{(n_{<} + \Delta n)!}} (i\eta)^{\Delta n} L_{n_{<}}^{\Delta n}(\eta^2). \quad (2)$$

Here  $\eta = kx_0 = k\sqrt{\hbar/2m\omega}$  is the Lamb-Dicke parameter for the spatial extension  $x_0$  of the ground state,  $n_{<}$  the smaller of the two numbers  $n$  and  $n'$ ,  $\Delta n = |n - n'|$ , and  $L_n^m$  denotes the generalized Laguerre polynomial. In the case of high vibrational excitation  $n, n' \gg 1$ ,  $U_{n',n}$  can be approximated as

$$U_{n+\Delta n,n} \approx i^{\Delta n} J_{\Delta n}(2\eta\sqrt{n}), \quad (3)$$

with the Bessel function of  $n$ th order  $J_n$ . The argument of the Bessel function is the product of the wave number and the classical vibration amplitude of the highly excited state. This is also the result that one would expect for the frequency-modulated spectrum of a classical oscillator. For big arguments  $\beta$  among the Bessel functions  $J_n(\beta)$  those of order  $n \approx \beta$  have the biggest modulus. Consequently, during the initial stages of cooling it is most efficient to tune the laser so that it induces transitions with  $\Delta n \approx 2\eta\sqrt{n} \gg 1$ .

For the final stages of cooling one can usually assume that the ion is in the Lamb-Dicke regime, i.e., that it is localized in a volume smaller in extent than the optical wavelength. A detailed study of the limits of sideband cooling in a static trap has been given by Javanainen *et al.* [15]. The final distribution of population over the vibrational states is thermal and can be characterized by a mean occupation number  $\langle n \rangle$  or a temperature  $T = \hbar\omega/k_B \ln(1 + 1/\langle n \rangle)$ . The number  $\langle n \rangle$  is a rational function of the four frequencies involved, i.e., the natural linewidth  $\Gamma$ , the oscillation frequency in the trap  $\omega$ , the laser detuning  $\delta$ , and the Rabi frequency  $\omega_R$ . For certain limiting cases simple expressions for  $\langle n \rangle$  can be derived from the general result given in [15]: The lowest vibrational excitation is achieved in the case of well-resolved sidebands ( $\omega \gg \Gamma$ ) and under weak laser excitation ( $\omega_R \ll \Gamma$ ), tuned to the first sideband ( $\delta = -\omega$ ):

$$\langle n \rangle = \left( \alpha + \frac{1}{4} \right) \frac{\Gamma^2}{4\omega^2}. \quad (4)$$

The constant  $\alpha$  depends on the geometry of excitation and photon reemission and is of the order of 1. In the case of strong saturation ( $\omega_R \gg \Gamma$ ) of the first sideband ( $\delta = -\omega$ ) the final energy is proportional to the laser intensity:

$$\langle n \rangle \approx \frac{\omega_R^2}{8\omega^2}. \quad (5)$$

This case is of practical relevance if one wants to detect a fluorescence signal on the cooling transition, e.g., to measure the internal state of the ion in a double-resonance experiment, while keeping the ion cold. For the choice of parameters  $\omega_R = \omega - \delta$ , the ion is still predominantly in the vibrational ground state ( $\langle n \rangle \approx 1/8$ ), but photons are scattered from the wing of the saturation-broadened carrier at a rate

$P = \Gamma \omega_R^2 / (\Gamma^2 + 2\omega_R^2 + 4\delta^2) \approx \Gamma/6$ , which is already one-third of the maximum scattering rate. Finally, in the case of big laser detuning ( $\delta \gg \Gamma, \omega, \omega_R$ ) the energy is proportional to the detuning since the lower vibrational levels are no longer depleted by the laser:

$$\langle n \rangle \approx \frac{\alpha + 1}{4} \frac{\delta}{\omega}. \quad (6)$$

If the Lamb-Dicke parameter satisfies  $\eta \ll 1$  the strength of the sidebands can be calculated from a power series expansion of the matrix elements in Eq. (2) and the thermal distribution of population over the oscillator levels. The  $U_{n',n}$  are evaluated to first order in  $\eta$  only. In this approximation, the height of the first lower-frequency sideband in the absorption spectrum relative to the carrier is  $\eta^2 \langle n \rangle$  and that of the first higher-frequency sideband  $\eta^2 (\langle n \rangle + 1)$ . This information can be used to determine experimentally the vibrational quantum number from the absorption spectrum [4,16]. The strengths of the higher-order sidebands contain higher powers of  $\eta^2$  and hence rapidly decrease.

Let us now briefly review some facts about the motional spectrum of an ion in a Paul trap [17,18], which is not just a static system but possesses an explicitly time-dependent potential. The equation of motion for a classical particle of charge  $e$  and mass  $m$  in the quadrupole potential of the trap  $\varphi(r,z) = (V_0 - U_0 \cos \Omega t)(r^2 - 2z^2)/2r_0^2$  is given by the Mathieu differential equation

$$\frac{d^2 r}{d\tau^2} + (a_r - 2q_r \cos 2\tau)r = 0, \quad (7)$$

with dimensionless parameters:

$$\tau = \frac{\Omega}{2} t, \quad a_r = \frac{4eV_0}{m\Omega^2 r_0^2}, \quad q_r = \frac{2eU_0}{m\Omega^2 r_0^2}. \quad (8)$$

Here a static voltage  $V_0$  and an alternating voltage with amplitude  $U_0$  and frequency  $\Omega$  are applied to a Paul trap with the radius of the ring electrode  $r_0$ . The equation of motion for the  $z$  coordinate is obtained by multiplying the parameters  $a$  and  $q$  by the factor  $-2$ . The general solution of the Mathieu equation in the first stability region of the  $(a, q)$  parameter space can be written by using the Floquet ansatz:

$$r(\tau) = A \sum_{j=-\infty}^{\infty} c_j \cos(2j + \beta_r)\tau + B \sum_{j=-\infty}^{\infty} c_j \sin(2j + \beta_r)\tau, \quad (9)$$

where  $A$  and  $B$  are constants determined by the initial conditions, and the  $c_j$  and  $\beta_r$  depend on  $a$  and  $q$ . In the first stability region the value of  $\beta_r$  is between 0 and 1. According to Eq. (9) the motional spectrum of the ion has resonances at

$$\omega_{r,j} = \left( j \pm \frac{\beta_r}{2} \right) \Omega, \quad j = 0, 1, 2, \dots \quad (10)$$

In the adiabatic approximation [18], which is valid for  $a, q^2 \ll 1$ , the movement of the ion can be separated into an oscillation at the driving frequency  $\Omega$ , the so-called micro-

motion, and a slower oscillation, called the secular motion, in the time-averaged pseudopotential. This pseudopotential describes the effect of the ponderomotive force of the oscillating trapping field that drives the ion to the field minimum at the center of the trap. Since in the quadrupole trap the pseudopotential is harmonic, the solution to the equation of motion can be approximated as

$$r(\tau) = r_0 \cos \beta_r \tau \left( 1 + \frac{q_r}{2} \cos 2\tau \right). \quad (11)$$

The approximate expression for  $\beta_r$  is  $\beta_r = \sqrt{q_r^2/2 + a_r}$ , and the secular frequencies are given by

$$\omega_r = \frac{\Omega}{\sqrt{8}} \sqrt{q_r^2 + 2a_r}, \quad \omega_z = \frac{\Omega}{\sqrt{2}} \sqrt{q_r^2 - a_r}, \quad (12)$$

which are the lowest-order resonances  $\omega_{r,z} = \beta_{r,z} \Omega/2$  in the Floquet ansatz, Eq. (9). From Eq. (11) it is seen that the amplitude of motion at the resonances  $\Omega \pm \omega$  is a factor  $q_r/4$  smaller than those at the resonance  $\omega$ . It is noteworthy that the frequency  $\Omega$  of the driving field does not appear directly in the motional spectrum, but only in combination with the secular frequency  $\omega$ . This changes, however, if there is an additional static force acting on the ion, displacing it from the center of the quadrupole. The approximate solution to the equation of motion then becomes

$$r(\tau) = (r_1 + r_0 \cos \beta \tau) \left( 1 + \frac{q_r}{2} \cos 2\tau \right) \quad (13)$$

and a resonance at  $\Omega$  appears. The force that displaces the ion by  $r_1$  may be due to static electric stray fields or the presence of a second ion in the trap. These effects can have a strong influence on sideband laser cooling of the trapped ions and will be treated in detail in Secs. IV and VI.

A number of theoretical studies have been conducted on the quantum-mechanical treatment of the Paul trap. The explicitly time-dependent potential does not allow stationary states with time-independent energy eigenvalues. One can, however, as in the case of the pseudopotential model, distinguish between two time scales and construct wave functions of the harmonic secular oscillator that show some additional breathing movement at the trap frequency [19,20]. A quantum-mechanical theory of sideband cooling in the time-dependent potential of the Paul trap exists only for special cases so far: Cirac *et al.* [21] treat predominantly the case where the ion is localized in the Lamb-Dicke regime at the node of a standing laser wave and have calculated time-averaged kinetic energies. They find minima of the energy that agree with the results of the theory for the static harmonic trap to within a factor of 2. The strongest modifications to the predictions of the cooling theory for the static trap arise in the dependence of the energy on the laser detuning: The influence of the micromotion gives rise to heating for certain ranges of negative laser detuning (on the high-frequency side of a low-frequency micromotion sideband) and to cooling for some positive detunings (on the low-frequency side of a high-frequency micromotion sideband). In Sec. IV we present experimental excitation spectra showing the heating regions for negative detuning and compare

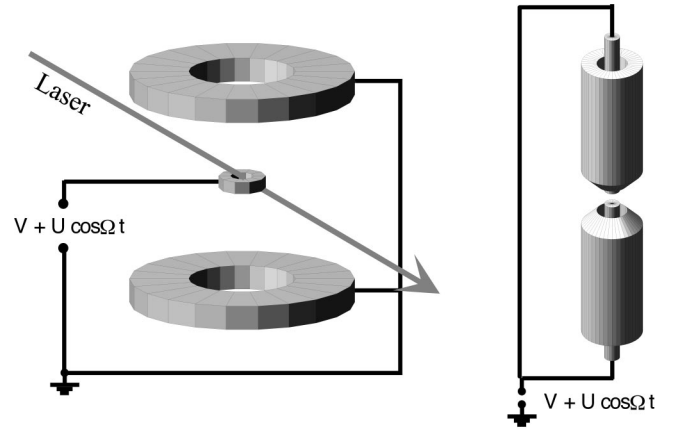


FIG. 1. Miniaturized radio-frequency ion traps. Left, Paul-Straubel trap (ring electrode with inner diameter 1 mm; drive frequency  $\Omega/2\pi = 10$  MHz at amplitude 1000 V). Right, end-cap trap (distance between the end caps 0.56 mm; drive frequency  $\Omega/2\pi = 14$  MHz with amplitude 200 V). For details see Ref. [24].

these results with a semiclassical theory that gives both the fluorescence rate and kinetic energy of the ion and that is also valid outside the Lamb-Dicke regime. In addition, the influence of micromotion due to the presence of a static field or a second ion is investigated.

### III. EXPERIMENT

We use miniaturized quadrupole radio-frequency traps that are geometrical variants of the original Paul trap and basically consist only of a ring electrode (Paul-Straubel trap [23]) or two endcaps (endcap trap [24]). The alternating and static trapping voltages are applied to these electrodes while the potential zero is defined by shield electrodes. In this way a field is created inside the ring or between the two endcaps, respectively, whose multipole expansion is dominated by the quadrupole contribution. These traps (see Fig. 1) are described in detail in Ref. [24]. They are relatively simple to fabricate in miniature size, making it easy to reach the Lamb-Dicke regime without having to apply high voltages. They are also geometrically quite open structures that allow good optical access to the trapped ion.

The experiments are performed with  $^{115}\text{In}^+$  ions that are sideband cooled through laser excitation of the  $5s^2\ ^1S_0 \rightarrow 5s5p\ ^3P_1$  intercombination line at a wavelength of 230.6 nm. In this transition the hyperfine component  $F \rightarrow F+1$  (where  $F=I=9/2$ ) is excited with circularly polarized light in vanishing magnetic field, so that optical pumping between the Zeeman sublevels results in a closed two-level system. The natural linewidth of the transition is  $\Gamma/2\pi = 360(30)$  kHz [8]. The laser radiation is produced by using a frequency-doubled stilbene-3 ring dye laser. To resolve the natural linewidth of the transition, the laser is frequency stabilized to a stable reference cavity by using a high-bandwidth electronic servo system. The laser linewidth is below 10 kHz. The saturation intensity of the cooling transition is  $I_S = 7.7$  mW/cm<sup>2</sup>, corresponding to a saturation power  $P_S = 0.23$   $\mu\text{W}$  for a focus area of  $3 \times 10^{-5}$  cm<sup>2</sup>. The laser system is capable of providing up to  $1000P_S$ . The resonance fluorescence emitted from the ion is detected using a

solar-blind photomultiplier. In all the experiments described below, laser excitation is performed with a single beam (sometimes containing two different frequencies). Cooling is nevertheless effective in all three dimensions because the laser wave vector has nonvanishing projections along all three major axes of the trap. In addition, the differences between the secular frequencies are comparable to the natural linewidth of the transition. It can thus be assumed that, irrespective of the precise value of the laser detuning, several sidebands corresponding to different vibrational degrees of freedom are always close to resonance with the laser. Under the experimental conditions described above, with typical secular frequencies  $\omega/2\pi = 1$  MHz and with  $\alpha = 1$  (cooling with one laser beam, but all degrees of freedom are assumed to be thermalized), Eq. (4) predicts a minimal mean occupation number  $\langle n \rangle = 0.04$  for the indium ion.

#### IV. INFLUENCE OF MICROMOTION

According to the adiabatic approximation the motion of an ion in a rf trap is composed of the high-frequency micromotion and the slower secular motion [see Eq. (11)]. While the micromotion amplitude depends on the position of the ion in the inhomogeneous field of the trap, the secular motion can be damped through laser cooling. In doing this, the ion spends less and less time in regions of high field strength and consequently the energy in the micromotion is reduced. For a single ion in a quadrupole trap without static potentials the time-averaged kinetic energies of micromotion and secular motion are equal. In the presence of electrostatic fields or when several ions are trapped simultaneously, the energy of the micromotion can be considerably higher than that of the secular motion. Limits of micromotion energy that are due to technical imperfections of the trap are calculated in [16]. In the case of laser-cooled Coulomb crystals of several ions [25,26] the final kinetic energy is completely dominated by the micromotion since the ions repel each other from the saddle point of the quadrupole potential. Micromotion has an influence on laser cooling because additional frequencies appear in the motional spectrum of the ion that are neglected in the approximation of the static harmonic trap. This gives rise to strong modifications in the dependence of the equilibrium energy of the ion on the laser detuning. In the case of Doppler cooling of weakly bound ions (where  $\omega < \Gamma$ ) this was first discussed in [27,28]. A quantum-mechanical theory of laser cooling in the strong binding regime taking into account the influence of micromotion was published by Cirac *et al.* [21]; however, not all the experimentally relevant cases were treated. In this section we present experimental results on cooling and heating processes that arise for negative detunings of the cooling laser and compare these with semi-classical calculations.

Figure 2 shows two experimental excitation spectra of the cooling transition  $^1S_0 \rightarrow ^3P_1$  of a single indium ion, obtained by tuning a single-frequency cooling laser. In Fig. 2(a) the laser was at 20-fold saturation intensity and static stray fields were not fully compensated so that some residual micromotion can be seen. At zero detuning the carrier of the spectrum shows an asymmetric line profile with a sharp drop in the fluorescence intensity as the detuning becomes positive. This is due to a rise in temperature because of nonresonant heat-

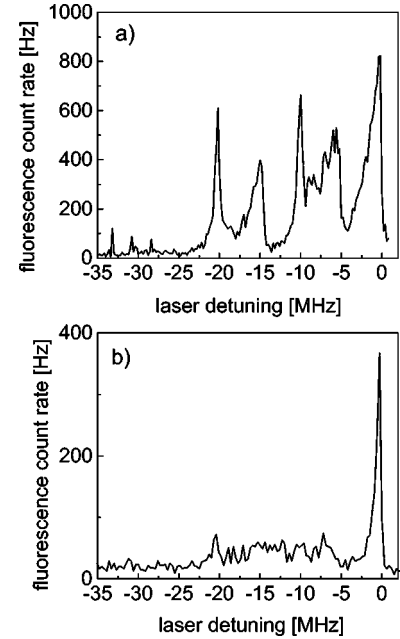


FIG. 2. Excitation spectrum of a single indium ion with monochromatic excitation. (a) With some residual micromotion through static stray fields (with an amplitude of about  $\lambda/10$ ) and with saturating laser excitation ( $I=20I_S$ ). Sidebands of the micromotion at  $\delta = -\Omega$  and  $\delta = -2\Omega$  are clearly visible ( $\Omega/2\pi = 10.02$  MHz). (b) With weaker laser excitation ( $I=4I_S$ ) and improved compensation of stray fields (amplitude of the micromotion below  $\lambda/20$ ).

ing on the high-frequency sidebands. Below resonance two prominent structures are visible: Starting from negative detuning, there is a sharp peak of the fluorescence intensity, then a wider region of elevated fluorescence followed by a rise and then by an abrupt decrease of the signal. The narrow peaks are at detunings corresponding to the first and second harmonics of the trap frequency  $\Omega$  (at  $-10$  MHz and  $-20$  MHz, respectively). The decrease of the fluorescence is at about the midpoint between the peaks. By applying dc voltages to compensation electrodes in the vicinity of the trap static stray fields can be canceled at the position of the ion. Changing these voltages leads to changes in the heights of the peaks at the trap frequency or finally to the disappearance of these peaks. This shows that they are sidebands of the residual micromotion. Since these sidebands are easily saturated in the excitation spectrum, this leads to an extremely sensitive method of detecting stray fields or other imperfections that cause micromotion in the trap: Let us assume that a sideband can be detected if it has 1% of the strength of the carrier. In an unsaturated spectrum this corresponds to a modulation index  $\beta = 2\pi a/\lambda \approx 0.2$ , where  $a$  is the amplitude of the motion of the ion along the laser beam with wavelength  $\lambda$  [since  $J_1^2(0.2) \approx 0.01, J_1$ : Bessel function of first order]. The minimal detectable amplitude would be about  $\lambda/30$ . Using the 100-fold saturation intensity would drive a sideband with  $J_1^2(\beta) = 0.01$  into saturation and make a sideband with  $J_1^2(\beta) = 0.0001$  detectable. This corresponds to an amplitude of  $\lambda/300$ , which would be smaller than the spread of the ground-state wave function in the present experiment. For the spectrum in Fig. 2(a), which was taken at  $I=20I_S$ , the unsaturated height of the first sideband is about  $J_1^2(\beta) = 0.1$ , corresponding to  $\beta=0.6$  or a micromotion amplitude

of  $\lambda/10$ . Before taking the spectrum in Fig. 2(b) the laser intensity was reduced to  $4I_S$  and the compensation of static fields was improved. An upper limit for the micromotion of  $\lambda/20$  can be deduced from this spectrum. The ion is localized well within the Lamb-Dicke regime and the carrier clearly dominates the spectrum.

To understand the structure of the excitation spectra, one has to consider the variations of the kinetic energy of the ion with the changing laser detuning. Each data point in Fig. 2 corresponds to an equilibrium situation where the ion is scattering at least  $10^3$  photons at fixed detuning. With every change of the detuning, however, the kinetic energy is altered. For laser detunings directly below micromotion sidebands very little fluorescence is observed, indicating that for these detunings the sidebands of the secular motion are only weakly excited and that this motion is well cooled. This is in qualitative agreement with the findings of Cirac *et al.* [21,22], who predict effective cooling for these detunings.

The spectral structures showing increased fluorescence for detunings on the blue side of the micromotion sidebands indicate higher excitation of the secular motion and less effective cooling. For this range of parameters the calculations presented in [21] give no results for the equilibrium energy or the shape of the excitation spectrum. To calculate these quantities we use the following model, in which the ion is treated as a classical particle: Let us first assume an ideal Paul trap without any additional micromotion caused by non-quadrupolar static fields. The solution of the one-dimensional Mathieu equation according to the Floquet ansatz, Eq. (9), is truncated after the first order, i.e., only terms  $j=0, \pm 1$  are considered. The motional spectrum of the ion thus consists of three resonances: one at the secular frequency  $\omega$  and two at the sum and difference frequencies  $\Omega \pm \omega$ , the latter with an amplitude that is a factor  $q/4$  smaller than those of the  $\omega$  term. Truncating the Floquet series after the first order is well justified since  $q \ll 1$  and the resonances  $j = \pm 2$  have an amplitude a factor  $q^2/64$  smaller than the term  $j=0$ . In the interaction with the laser light the frequency modulation due to the ion's motion will cause a comb of sidebands for each of the three frequencies. Besides the carrier, the absorption spectrum will show sidebands at detunings  $j\omega, j'(\Omega \pm \omega)$ , and — via mixing of the frequencies — also  $j'\Omega \pm j\omega$ . At a given laser detuning absorption can take place through sidebands of different order for different modulation frequencies. All processes that involve absorption on a low-frequency secular sideband  $j < 0$  will lead to cooling, all those involving a high-frequency secular sideband  $j > 0$  to heating. For the detuning  $\delta = -\Omega$ , for example, the laser is simultaneously in resonance with the first low-frequency  $\omega$  sideband of the first low-frequency ( $\Omega - \omega$ ) sideband — a cooling process — and with the first high-frequency  $\omega$  sideband of the first low-frequency ( $\Omega + \omega$ ) sideband — a heating process. It will also be assumed that the frequency ratio  $\Omega/\omega = m$  is an integer [29] so that for detuning  $-\Omega$  the laser is also in resonance with the  $m$ th low-frequency  $\omega$  sideband, an additional contribution to cooling which will become effective at higher excitation of the secular motion. The distinction between cooling and heating processes appears naturally by considering the laser spectrum in the rest frame of the ion: At the detuning  $\delta = -\Omega$ , for example, the laser sideband to the modulation frequency  $\Omega$

$-\omega$  is detuned by  $-\omega$  and consequently cools the ion. The sideband  $\Omega + \omega$  already has a positive detuning  $\omega$  and is heating. The change of the kinetic energy of the ion's secular motion that is produced through these various resonances is obtained from the product of the respective scattering rate and the detuning. In addition, each scattered photon increases the average energy of the ion by the photon recoil energy  $E_R = \hbar R$ , where  $R$  is the recoil frequency  $\hbar k^2/2m$ .

In calculating the absorption spectrum the ion is treated as an oscillator with amplitude  $a$  at frequency  $\omega$  and amplitudes  $aq_r/4$  at  $\Omega \pm \omega$ . The strength of a sideband corresponding to modulation order  $j$  of the secular motion, order  $j^+$  of the frequency  $\Omega + \omega$ , and order  $j^-$  of the frequency  $\Omega - \omega$  is given by the product of the squares of Bessel functions:  $J_j^2(\beta)J_{j^+}^2(\beta q_r/4)J_{j^-}^2(\beta q_r/4)$ , where  $\beta = 2\pi a/\lambda$  is the modulation index of the secular motion. From the amplitude of the secular motion the mean secular kinetic energy  $E = ma^2\omega^2/2$  is calculated. This classical model is justified in the heating regions, because here the vibrational energy of the ion increases to several hundred  $\hbar\omega$ . Here the model gives a good approximation for the strengths of the sidebands calculated in a fully quantum-mechanical treatment [see Eq. (3)]. In the cooling regions the model predicts energies smaller than  $\hbar\omega$ , showing that the classical treatment is no longer valid. However, if a quantum number  $\langle n \rangle = E/\hbar\omega$  is calculated, this is in reasonable agreement with the quantum-mechanical theory of Javanainen *et al.* [15]. In this theory of the static harmonic trap thermal excitation of oscillator levels is found as a result of laser cooling. The corresponding absorption spectrum would show a Gaussian envelope of sidebands. In our model of the time-dependent Paul trap the ion's oscillation is not in thermal equilibrium and is characterized by its amplitude. This leads to a different form of the absorption spectrum, especially for modulation indices bigger than two, where the Bessel functions show first zeroes. We tried both shapes of the absorption spectrum and found that the experimental structure of the excitation spectrum in the heating regions is much better reproduced by the model with the Bessel function spectrum. The model with the Gaussian spectrum shows more of a steplike-modulated excitation spectrum without the second fluorescence maximum in each structure. The results for the equilibrium kinetic energy do not differ much between the two models. The choice of model is motivated by the comparison with the experimental result. In experiments with weakly bound ions under the influence of micromotion high-amplitude nonthermal oscillations have previously been observed [28,30].

Figure 3 shows the result for the numerical calculation of the equilibrium kinetic energy and fluorescence intensity as a function of laser detuning. The parameters were chosen to approximate those of the indium experiments,  $q_r = 0.2$ ,  $\Omega/\omega = 10$ ,  $\Gamma/\omega = 0.36$ ,  $R/\omega = 0.032$ , and the laser intensity was assumed to be well below saturation. To simplify the calculation the effect of the finite linewidth  $\Gamma$  is neglected and only resonant excitations were calculated for values of the detuning  $\delta = -j\omega$ ,  $j = 1, 2, 3 \dots$ . Nonresonant scattering was considered only for the carrier since this process determines the line shape close to  $\delta = 0$  and the minimal energy in the cooling regions.

The most prominent feature of this calculation is the heat-

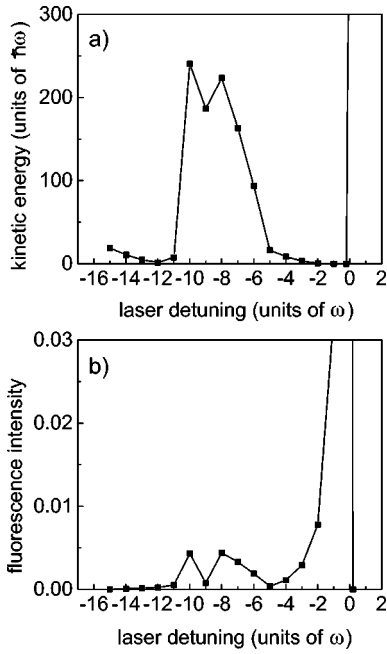


FIG. 3. Numerical simulation of sideband cooling in a Paul trap. (a) Mean kinetic energy of the secular motion; (b) fluorescence intensity as a function of laser detuning. The unit for the fluorescence intensity is the emission of the cold ion at resonance. Parameters: drive frequency  $\Omega = 10\omega$ ,  $q_r = 0.2$ .

ing region for detunings  $-10\omega < \delta < -5\omega$ . In this region there are two maxima of the mean kinetic energy at  $\delta = -\Omega$  and  $\delta = -\Omega + 2\omega$ , corresponding to laser detuning on the first secular sideband above the motional frequencies  $\Omega - \omega$  and  $\Omega + \omega$ , respectively. In the excitation spectrum this leads to small peaks of the fluorescence intensity at the same detunings. The mean kinetic energy of about  $200\hbar\omega$  is far above the minimal value that is achievable at the detuning  $\delta = -\omega$ , but on an absolute scale this energy is still small: expressed in temperature units  $200\hbar\omega$  corresponds to only  $k_B \times 10$  mK for  $\omega/2\pi = 1$  MHz.

In this heating region at negative detuning the system is multistable, i.e., there are several values of the oscillation amplitude that give stable equilibrium between heating and cooling. For the calculation shown in Fig. 3 the laser approached the resonance starting from negative detuning — as is done in the experiment — and the state of the ion was iterated from one detuning to the next. The solutions found in this way were always the equilibrium situations of the lowest energy. However, once the ion is heated up to higher energy, it will not be cooled down again to the state of the lowest energy but can remain in a stable situation at higher oscillation amplitude. Our model also possesses stable solutions of low energy for positive values of the detuning in the range  $6\omega < \delta < 10\omega$ , similar to those predicted by Cirac *et al.* [21]. These states will not, however, be reached when the cooling laser is continuously tuned over the carrier, since the ion will strongly heat up at the detuning  $\delta = \omega$ . Outside the Lamb-Dicke regime there is no useful sideband cooling in regions of positive detuning. These results of the calculations are in agreement with the experimental observations.

Let us now turn to the case of additional micromotion due to, for example, an additional static field that breaks the

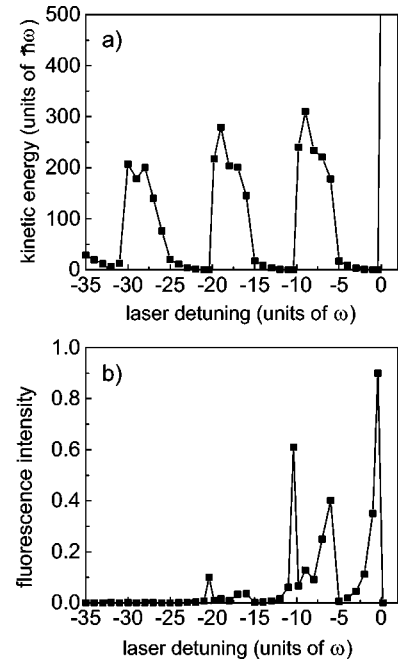


FIG. 4. Numerical simulation of sideband cooling in a Paul trap in the presence of additional micromotion. (a) Mean kinetic energy of the secular motion; (b) fluorescence intensity as a function of laser detuning. The parameters are approximately those of the experimental spectrum shown in Fig. 2(a) ( $\Omega = 10\omega$ ,  $q_r = 0.2$ , micromotion amplitude  $\lambda/10$ ).

quadrupole symmetry, as is the case in the spectrum in Fig. 2(a). Since this additional micromotion has a fixed amplitude that is not reduced through laser cooling, it is treated like a fixed frequency modulation of the laser, i.e., we transform to a reference system that follows the micromotion. With this laser spectrum, the same model as described above is used to calculate the average kinetic energy and the shape of the excitation spectrum. The result is shown in Fig. 4, where a micromotion modulation index of 0.6 was assumed, corresponding to an oscillation amplitude of  $\lambda/10$ . Only the first two pairs of sidebands at  $\pm\Omega$  and  $\pm 2\Omega$  were taken into account. Through the strong excitation at  $I = 20I_S$  the sidebands in the excitation spectrum appear more pronounced relatively to the carrier. The form of the calculated excitation spectrum is in good agreement with the experimental result of Fig. 2(a): Below resonance there are two structures of increased fluorescence, each of them showing a maximum at the beginning and the end of a region of laser detunings with elevated kinetic energy of the ion. The contribution of the sideband  $\delta = -2\Omega$  is underestimated in the model in relation to the experiment, indicating that the second harmonic of the trap frequency may also contribute to the frequency modulation, perhaps because of the curvature of the ion's trajectory.

In this section we presented an experimental and theoretical investigation of the influence of micromotion on sideband cooling of an ion in a radio-frequency trap. The interaction of the ion with the laser radiation leads to a more complex dynamics than one would expect in the case of a static harmonic trap. Together with the time-dependent trap potential, a laser that is tuned below the resonance of the free ion can under certain conditions increase the ion's kinetic energy. On the other hand, there are also regions of detun-

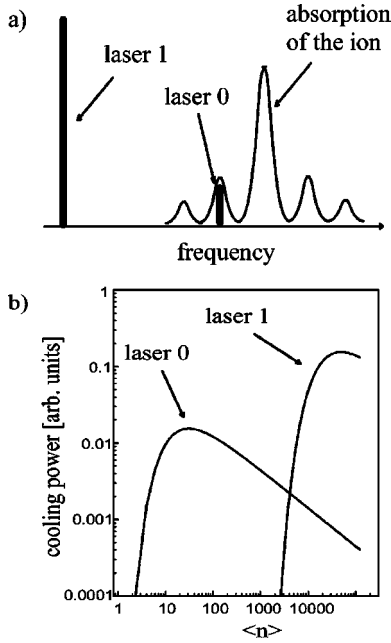


FIG. 5. (a) Scheme of bichromatic sideband cooling: The strong laser 1 is far detuned and ensures efficient cooling for higher vibrational excitation while the weaker laser 0 allows cooling to the vibrational ground state on the first low-frequency sideband. An excitation spectrum of the ion can be recorded by scanning laser 0 across the carrier. (b) Relative cooling power for the two lasers as a function of the vibrational excitation (parameters are those of the experiment in Fig. 6).

ings where the minimal kinetic energy is comparable to or even smaller than the value expected in the approximation of a static trap.

## V. BICHROMATIC SIDE BAND COOLING OF A SINGLE ION

According to the theory [15] the lowest temperatures are expected if the cooling laser is tuned to the first low-frequency secular sideband with an intensity well below saturation. Under these conditions very little fluorescence is emitted and, should the ion temporarily heat up after a collision with a residual-gas molecule, the cooling power for the hot ion is small because of the small detuning. To provide faster cooling at higher temperatures and, furthermore, be able to record high-resolution spectra of the cooling transition in the Lamb-Dicke regime, the method of bichromatic sideband cooling was developed (see Fig. 5): Cooling is performed with two lasers of different frequency and intensity. A strong laser (called laser 1) is tuned to a low-frequency sideband of high order and produces nearly no fluorescence from the cold ion. This laser is responsible for effective cooling from higher vibrational levels, should these become excited. At the same time a weak laser (laser 0) is tuned to the first red secular sideband to provide cooling to low vibrational quantum numbers, or can also be tuned across the carrier to record a spectrum while the far detuned laser ensures continuous cooling. These spectra will be used later to determine the temperature of the ion.

The presence of laser 1 has an influence on the minimal achievable temperature since at low vibrational quantum

numbers it practically does not contribute to the cooling, but produces some heating through nonresonant photon scattering. To estimate the minimum vibrational quantum number let us consider the problem in the approximation of a static harmonic trap. It is assumed that laser 0 with intensity  $I_0 \ll I_S$  is tuned to the first red sideband ( $\delta_0 = -\omega$ ), while laser 1 with intensity  $I_1 > I_0$  is in resonance with the  $l$ th red sideband ( $\delta_1 = -l\omega$ ). The sideband of order  $j$  and with strength  $S_j$ , excited with a laser of intensity  $I$ , will scatter photons at the rate

$$P_j = \frac{\Gamma^3 S_j I / I_S}{\Gamma^2 (1 + 2S_j I / I_S) + 4\delta_j^2}, \quad (14)$$

where  $\delta_j = (\omega_L - \omega_0 - j\omega)$  is the detuning of the laser with frequency  $\omega_L$  from the  $j$ th sideband of the atomic resonance  $\omega_0$ . The heating and cooling powers through scattering processes on the different sidebands can be estimated as follows: Every absorption on a red sideband  $-l$  will reduce the vibrational energy by  $l\hbar\omega$ , while every absorption on a blue sideband  $l$  heats the ion by  $l\hbar\omega$ . Every absorption on the carrier increases the energy of the ion on the average by  $\alpha$  times the recoil energy  $\hbar R$ . Since  $R$  is much smaller than  $\omega$  (for the indium ion:  $R/2\pi = 32.6$  kHz and  $\omega/2\pi \approx 1$  MHz;  $\eta^2 \approx 0.03$ ), recoil heating through scattering on the sidebands is neglected. It is also assumed that  $\langle n \rangle < 1$  and  $\eta^2 \ll 1$ , and only scattering on the carrier and on the first-order sidebands  $j = \pm 1$  is considered. Only one-photon processes are taken into account, i.e., the interactions of the ion with the two laser beams are treated independently of one another. The main influence of the strong and far detuned laser 1 is to produce a small light shift of the atomic frequency  $\omega_0$  that can easily be compensated for by a slight change in the frequency of laser 0. The intensity  $I_1$  can be bigger than the saturation intensity  $I_S$ , but  $(1 + 2I_1/I_S) < 4l^2\omega^2/\Gamma^2$  should hold, so that the scattering rate that this laser produces through nonresonant excitation of the carrier is well below  $\Gamma/2$ . Using these approximations, one can write the equilibrium between heating and cooling processes as

$$\begin{aligned} \frac{I_0}{I_S} \Gamma \langle n \rangle \eta^2 \omega + \frac{I_1}{I_S} \frac{\Gamma^3}{4(l-1)^2 \omega^2} \langle n \rangle \eta^2 \omega \\ = \frac{I_0}{I_S} \frac{\Gamma^3}{4\omega^2} \alpha R + \frac{I_0}{I_S} \frac{\Gamma^3}{16\omega^2} \langle n+1 \rangle \eta^2 \omega + \frac{I_1}{I_S} \frac{\Gamma^3}{4l^2 \omega^2} \alpha R \\ + \frac{I_1}{I_S} \frac{\Gamma^3}{4(l+1)^2 \omega^2} \langle n+1 \rangle \eta^2 \omega. \end{aligned} \quad (15)$$

Since  $\langle n \rangle < 1$ ,  $l \gg 1$ , and  $R = \eta^2 \omega$ , the expression can be simplified to yield

$$\langle n \rangle = \frac{\Gamma^2}{4\omega^2} \left( \alpha + \frac{1}{4} + \frac{I_1}{I_0} \frac{\alpha + 1}{l^2} \right). \quad (16)$$

For  $I_1 \rightarrow 0$  Eq. (4) is recovered. Typical parameters of the indium experiments are  $l = 40$ ,  $I_1 = 1000I_0$ ,  $\Gamma^2/\omega^2 = 0.13$ , and  $\alpha = 1$ . In this case  $\langle n \rangle$  increases from 0.041 in the optimal monochromatic case to 0.081 in the case of bichromatic sideband cooling. However, the cooling power for higher vibrational quantum numbers  $n > l$  is increased by roughly

the factor  $I_S/I_0$  (for  $I_1 > I_S$ ), which is about 400 for our typical experimental parameters [see Fig. 5(b)].

To record an excitation spectrum of the cooling transition the weak laser 0 can be scanned across the carrier. The cooling power from this laser will drop and the temperature will rise until cooling through laser 1 becomes effective. According to Eq. (6) this is expected for  $\langle n \rangle \approx 1/2$ . Since two laser frequencies can contribute to the fluorescence signal, it might be asked whether the relative strength of the first low-frequency sideband to the carrier is simply given by  $\langle n \rangle \eta^2$  and can be used to determine  $\langle n \rangle$ . As laser 0 is in resonance with the first red sideband,  $\langle n \rangle < 1$  and some resonant scattering is observed with amplitude  $\Gamma \langle n \rangle \eta^2 I_0/I_S$ . With laser 0 in resonance with the carrier, the quantum number  $\langle n \rangle$  rises to  $1/2$  and the scattering rate of laser 1 from the sidebands will increase slightly, while the strength of the carrier for the resonant laser 0 is somewhat reduced. Both effects are small as long as the ion stays in the Lamb-Dicke regime ( $\sqrt{n} \eta < 1$ ), which is fulfilled in the experiment. The contribution from laser 1 to the carrier resonance curve is small because laser 0 can scatter on the average  $\omega/R \approx 30$  photons until the energy of the ion is increased by one vibrational quantum, which can subsequently be extracted by one additional photon from laser 1. So the spectrum obtained in this way quite closely resembles the unsaturated spectrum of the ion at fixed temperature and the ratio of the strength of the red sideband to the carrier is given by  $\langle n \rangle \eta^2$  for the minimal vibrational quantum number.

In the theoretical treatment presented so far the time dependence of the potential of the Paul trap has been neglected. As shown in the preceding section, it has an important influence on the absorption spectrum of the ion. The far detuned laser can excite not only secular frequency sidebands of high order but also secular frequency sidebands of the micromotion, leading to stronger interaction of this laser with the ion. As can be seen from Eq. (16), a smaller effective detuning of laser 1 will lead to a higher-temperature limit. The detuning has to be chosen on the low-frequency side of a micromotion sideband to avoid the heating regions identified in the preceding section. The presence of micromotion sidebands will improve the stability of bichromatic cooling for high temperatures, as more laser frequencies are added to the cooling curve shown in Fig. 5(b). Also, while laser 0 is scanned over the carrier the ion will heat up less because of the smaller effective detuning of laser 1.

The experimental result with a single ion in the Paul-Straubel trap is shown in Fig. 6. For the actual realization of bichromatic sideband cooling, a single laser beam was used that was passed through an electro-optical modulator with variable modulation frequency. Through phase modulation two weak sidebands containing about 0.001 of the total power each were created around the original laser frequency. The carrier of this spectrum served as laser 1 and was detuned by about  $-40$  MHz, corresponding to  $-40\omega$  or  $-110\Gamma$ . This beam had about 200 times the saturation intensity. The high-frequency phase modulation sideband was used as laser 0 and was tuned by changing the drive frequency of the electro-optical modulator. This method simultaneously produces a weak sideband at  $-80$  MHz detuning, whose influence on the ion can be neglected. The data in Fig. 6 were fitted by a single Lorentzian curve with a constant

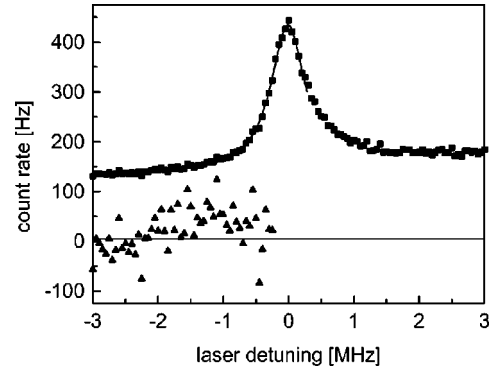


FIG. 6. Excitation spectrum of a single indium ion with bichromatic sideband cooling. Power in laser 1,  $43 \mu\text{W}$ ; in laser 0, about  $30 \text{ nW}$ ; detuning of laser 1,  $-42 \text{ MHz}$ . Below, deviations between the data and the fitted Lorentzian curve in tenfold magnification.

background. The width of this Lorentzian is  $650 \text{ kHz}$  and lies above the natural linewidth of  $360 \text{ kHz}$ , indicating some saturation broadening and a slight drift of the resonance frequency due to a changing light shift from laser 1 (32 spectra were averaged over a total measurement time of 2 h). The deviations of the data from the fit are shown in the lower part of Fig. 6 in tenfold magnification. In the region of laser detunings corresponding to the secular frequencies ( $880$ ,  $950$ , and  $1450 \text{ kHz}$ ; these frequencies were measured for identical trap parameters by electronically exciting a cloud of trapped ions) an increase of the signal by about  $2(1)\%$  of the height of the Lorentzian is observable. The wing of the Lorentzian for positive detuning in Fig. 6 shows a raised fluorescence level. This is due to the heating that is produced by laser 0 as it is scanned over the blue sidebands. For these detunings the temperature and the scattering rate are higher. The sideband structure can also be made clearly visible by increasing the power in laser 0 to enhance the heating.

Since the three secular frequencies are not well resolved, an exact analysis of the three-dimensional situation and the partition of the vibrational energy is not possible. We therefore determine a mean vibrational quantum number in a spherically symmetric oscillator potential with an average frequency  $\omega/2\pi = 1090 \text{ kHz}$ . This gives an estimate of the average quantum number for the three vibrational modes of the ion. With  $\eta = k\sqrt{\hbar/2m\omega} = 0.174$  and a relative strength of the red sideband of  $0.02(1)$  the result for this quantum number is  $\langle n \rangle = 0.7(3)$ , corresponding to a temperature of about  $60 \mu\text{K}$ . This result indicates that the ion is in the vibrational ground state with a probability exceeding 50% for a basically unlimited time duration (several minutes in the actual experiment). In this respect the experiment is different from previous demonstrations of ground-state sideband cooling [4,5], where states with low quantum numbers  $\langle n \rangle \approx 0.05$  were produced at the end of a cooling sequence, but were also rapidly destroyed through the state measurement itself or parasitic heating processes.

Theory predicts much lower quantum numbers  $\langle n \rangle \approx 0.08$  [see Eq. (16)] for sideband cooling of the indium ion. This discrepancy may be attributed in part to this theory that neglects the influence of micromotion, but it may also be due to the limited experimental sensitivity. A problem of the experiment is that the sidebands in the spectrum of the cooling transition are not completely resolved, making it difficult to

measure these low temperatures from the strength of the sidebands. However,  $\text{In}^+$  also possesses the narrow  $^1S_0 \rightarrow ^3P_0$  transition, which is a favorable candidate for an optical frequency standard [8]. A double-resonance experiment [31] will allow more precise temperature determination using the much better resolved sidebands of this transition. In this spectrum the sidebands can also be saturated and detected more sensitively [16] without impairing the cooling through too strong excitation of the cooling transition. This would allow an experimental test of the limits of sideband cooling under various conditions.

## VI. COOLING OF COULOMB CRYSTALS

The formation of Coulomb crystals of laser-cooled ions — rigid structures of equally charged ions held together by the trap — was first observed with weakly bound ions in small Paul traps [25,26]. The crystallization of a strongly coupled plasma is expected when the ratio of Coulomb energy to thermal energy  $\Gamma_c = e^2 / (4\pi\epsilon_0 d k_B T)$  reaches a value of about 150 [32]. For a typical interion distance  $d$  of 10  $\mu\text{m}$  this happens at a temperature of 11 mK, a value easily accessible with Doppler cooling. However, for a vibrational frequency of typically 1 MHz this energy still corresponds to a vibrational excitation  $\langle n \rangle \approx 200$ , so that the mechanical behavior of these crystals is basically classical. The question arises whether it is possible to bring such a Coulomb crystal to the quantum ground state of all its vibrational modes by using the more efficient sideband cooling method. The interest here is to create a mesoscopic quantum object consisting of several separable atoms in one common quantum state.

For an experimental realization of a quantum Coulomb crystal some difficulties have to be overcome: With the number of ions in the crystal the number of vibrational modes that have to be cooled at different frequencies increases. In a Paul trap the ions in the crystal will also show strong phase-coupled micromotion with a kinetic energy far exceeding that of the thermal secular motion. To circumvent this problem, two-dimensional quadrupole traps (i.e., storage rings [33] or linear traps [34]) were considered to be the more suitable systems to cool a Coulomb crystal to the quantum regime. In such a trap a linear chain of ions can be trapped along the field-free axis without any micromotion. A strong motivation for the experimental realization of such a system came from the proposal to use the chain of ions as the register of a quantum computer [12], where each ion represents one quantum bit and the coupling between the ions is mediated by the common center-of-mass motion of the crystal, which, however, has to be cooled to the motional ground state as an initial condition. A disadvantage of the linear trap is the relatively low axial frequency, which makes it less efficient to cool this degree of freedom. So far cooling of small Coulomb crystals to the quantum regime has only been successful in miniature quadrupole traps that lead to strong binding in all three directions: in the experiment reported recently in [35] and in the experiment reported here. The NIST group [35] used a quadrupole trap with elliptic ring electrode that allows short chains of ions to be trapped along the longer axis of the ring. Two  $\text{Be}^+$  ions were cooled to near the vibrational ground state by pulsed Raman sideband cooling. The experiment described here uses bichromatic

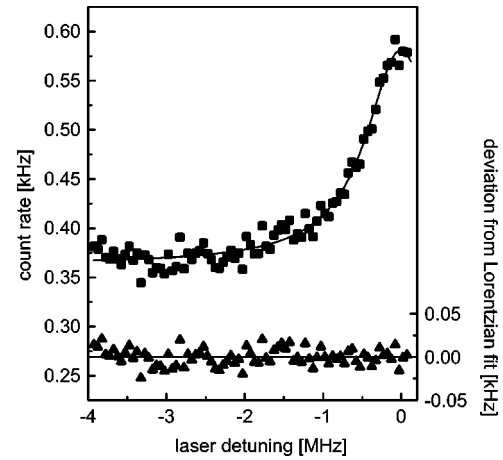


FIG. 7. Excitation spectrum of a two-ion Coulomb crystal with bichromatic cooling. Power in laser 1, 280  $\mu\text{W}$ ; in laser 0, about 50 nW; detuning of laser 1,  $-72$  MHz. Below, deviations between the data and the fitted Lorentzian.

sideband cooling of two  $\text{In}^+$  ions in a miniature endcap trap (see Fig. 1). First experiments on laser cooling of two-ion crystals of indium on the narrow intercombination line  $^1S_0 \rightarrow ^3P_1$  have already been reported in [36], but under conditions where the laser linewidth did not allow full resolution of the sideband structure.

In the new experiment two ions are stored in the endcap trap with parameters  $\Omega/2\pi = 13.78$  MHz,  $q_r = 0.14$ , leading to secular frequencies of 810 kHz in the radial direction and 1250 kHz along the trap axis. The two ions are located in the radial plane  $z = 0$ . Because of tolerances in the assembly of the trap we assume that the radial frequencies are not exactly degenerate but differ by a few percent. The direction of the weaker axis along which the ions are aligned is not known *a priori*, but the crystal is not rotating since there is no torque acting on the ions. The distance between the ions is  $d = 4.5$   $\mu\text{m}$ , as calculated in the pseudopotential model from the radial frequency. The amplitude of micromotion along the crystal axis is  $q_r d/4 = 160$  nm, resulting in a maximal modulation index of 4.3 for a cooling laser directed along this axis. Because of this strong micromotion the excitation spectrum of the cooling transition under monochromatic excitation shows strong heating regions above the low-frequency micromotion sidebands as discussed in Sec. IV, but also efficient cooling for detunings below these sidebands. We use the method of bichromatic sideband cooling and tuned laser 1 slightly below the fifth micromotion sideband. Compared with the single-ion experiments described in Sec. V, it was necessary to increase the laser intensity to about  $1000I_S$  in order to obtain long-term stable cooling. An excitation spectrum obtained by tuning the weak laser 0 revealed three prominent micromotion sidebands below the carrier. This indicates that the effective micromotion modulation index is about 2 and that the crystal is oriented in the radial plane at an angle of  $60^\circ$  to the laser beam, which forms an angle of  $20^\circ$  with the radial plane. Figure 7 shows an excitation spectrum of the two-ion crystal in the vicinity of the carrier, averaged over 11 scans.

To analyze the spectrum we have to consider the vibrational degrees of freedom of the two-ion crystal in the pseudopotential [26,35,37]. There are three center-of-mass

modes (in-phase movement of the two ions) with frequencies  $\omega_x$ ,  $\omega_y$ , and  $\omega_z$ . (Let  $\omega_x$  be the smaller of the two radial frequencies, so that the crystal is aligned along the  $x$  axis.) In addition, there is the axial breathing mode (out-of-phase movement) at frequency  $\omega_{xx} = \sqrt{3}\omega_x$  and two modes of out-of-phase vibration perpendicular to the  $x$  axis with frequencies  $\omega_{xy} = (\omega_y^2 - \omega_x^2)^{1/2}$  and  $\omega_{xz} = (\omega_z^2 - \omega_x^2)^{1/2}$ . Since  $\omega_{xy} < \Gamma$ , this mode is not resolved in the excitation spectrum and will not be cooled to  $\langle n_{xy} \rangle < 1$ , but only to the Doppler limit  $\langle n_{xy} \rangle \approx \Gamma/2\omega_{xy}$ . The motional spectrum should consist of resonances at  $\omega_x \approx \omega_y = 2\pi \times 810$  kHz,  $\omega_{xz} = 2\pi \times 950$  kHz,  $\omega_z = 2\pi \times 1250$  kHz, and the breathing mode  $\omega_{xx} = 2\pi \times 1400$  kHz. The experimental data were fitted with a single Lorentzian resonance curve centered on the carrier frequency. The lower curve in Fig. 7 shows the deviations of the data from this fit. The noise level is somewhat higher than in the case of the single-ion experiment because of the higher intensity in laser 1, which leads to a higher stray light intensity, and because of the shorter total measurement time. The data show no systematic increase of the fluorescence in the range of detunings corresponding to the vibrational frequencies. An upper limit for the relative strength of the motional sidebands can be derived from the noise level of 4%. As in the analysis of the single-ion experiment in Sec. V, we will only determine an average vibrational quantum number for all degrees of freedom with a mean frequency of 1040 kHz. With  $\eta = 0.177$  the result is  $\langle n \rangle < 0.04/\eta^2 = 1.3$ . Within the experimental uncertainty, the vibrational quantum number achieved with the two-ion crystal was as low as that with the single ion. The crystal is in the ground state for five of its six modes with about 50% probability over long time scales. The total kinetic energy of the micromotion  $m\Omega^2(q,d)^2/16$  is four orders of magnitude higher than the energy of the

secular motion. This indicates appreciable decoupling between the two motions.

With increasing number of ions in the crystal the proportion of the micromotion energy will increase, so that, if scaling to higher ion numbers is desirable — as for the register of a quantum computer — a micromotion-free linear or ring trap will be the better suited system. Although the indium ion can be laser cooled very effectively, it is not a very favorable candidate for realizing a quantum computer following the proposal of Cirac and Zoller [12], since it does not possess a suitable internal degree of freedom with sufficiently long coherence time. The ground state has no hyperfine structure and the lifetime of the metastable  $^3P_0$  level is only 140 ms [8], probably too short for more complex quantum logic operations. It is conceivable, however, to use a linear chain consisting of ions of two different elements where  $^{115}\text{In}^+$  would be used for cooling and a second, preferentially lighter, ion such as  $^{25}\text{Mg}^+$  would represent the quantum bit in its ground-state hyperfine structure. Both ions are strongly coupled via the Coulomb interaction and form a single crystal with eigenmodes involving both elements. These can be cooled even though only the indium ions are excited by the cooling laser. In this scheme the cooling does not affect the state of the quantum bits so that additional flexibility is obtained in the sequence of cooling and logic cycles in a quantum algorithm. In addition, the indium ions serve as “spacers” between the quantum bits and would facilitate their individual addressing through focused laser beams.

#### ACKNOWLEDGMENTS

We thank W. Lange for discussions about the possible implications for quantum computation, and A. Rusch for his contributions to the experimental setup.

- 
- [1] D. Wineland and H. Dehmelt, *Bull. Am. Phys. Soc.* **20**, 637 (1975).
  - [2] D.J. Wineland and W.M. Itano, *Phys. Rev. A* **20**, 1521 (1979).
  - [3] T.W. Hänsch and A.L. Schawlow, *Opt. Commun.* **13**, 68 (1975).
  - [4] F. Diedrich, J.C. Bergquist, W.M. Itano, and D.J. Wineland, *Phys. Rev. Lett.* **62**, 403 (1989).
  - [5] C. Monroe, D.M. Meekhof, B.E. King, S.R. Jefferts, W.M. Itano, D.J. Wineland, and P. Gould, *Phys. Rev. Lett.* **75**, 4011 (1995).
  - [6] H. Perrin, A. Kuhn, I. Bouchoule, and C. Salomon, *Europhys. Lett.* **42**, 395 (1998).
  - [7] S.E. Hamann, D.L. Haycock, G. Klose, P.H. Pax, I.H. Deutsch, and P.S. Jessen, *Phys. Rev. Lett.* **80**, 4149 (1998).
  - [8] E. Peik, G. Hollemann, and H. Walther, *Phys. Rev. A* **49**, 402 (1994).
  - [9] H. Dehmelt, *IEEE Trans Instrum. Meas.* **31**, 83 (1982).
  - [10] D.M. Meekhof, C. Monroe, B.E. King, W.M. Itano, and D.J. Wineland, *Phys. Rev. Lett.* **76**, 1796 (1996); **77**, 2346(E) (1996).
  - [11] C. Monroe, D.M. Meekhof, B.E. King, and D.J. Wineland, *Science* **272**, 1131 (1996).
  - [12] J.I. Cirac and P. Zoller, *Phys. Rev. Lett.* **74**, 4091 (1995).
  - [13] C. Monroe, D.M. Meekhof, B.E. King, W.M. Itano, and D.J. Wineland, *Phys. Rev. Lett.* **75**, 4714 (1995).
  - [14] S. Stenholm, *Rev. Mod. Phys.* **58**, 699 (1986).
  - [15] J. Javanainen, M. Lindberg, and S. Stenholm, *J. Opt. Soc. Am. B* **1**, 111 (1984).
  - [16] D. Wineland, W. Itano, J. Bergquist, and R. Hulet, *Phys. Rev. A* **36**, 2220 (1987).
  - [17] R.F. Wuerker, H. Shelton, and R.V. Langmuir, *J. Appl. Phys.* **30**, 342 (1959).
  - [18] H. Dehmelt, in *Advances in Atomic and Molecular Physics*, edited by D. R. Bates and I. Estermann (Academic, New York, 1967), Vol. 3; *ibid.* (Academic, New York, 1969), Vol. 5.
  - [19] L.S. Brown, *Phys. Rev. Lett.* **66**, 527 (1991).
  - [20] R. Glauber, in *Proceedings of the International School of Physics “Enrico Fermi,”* edited by E. Arimondo and W. Phillips (North-Holland, Amsterdam, 1991), Vol. 118.
  - [21] J.I. Cirac, L.J. Garay, R. Blatt, A.S. Parkins, and P. Zoller, *Phys. Rev. A* **49**, 421 (1994).
  - [22] For a comparison with our results see especially Fig. 3(b) of Ref. [21], which shows the case of traveling-wave laser excitation.
  - [23] N. Yu, W. Nagourney, and H. Dehmelt, *J. Appl. Phys.* **69**, 3779 (1991).

- [24] C. Schrama, E. Peik, W.W. Smith, and H. Walther, *Opt. Commun.* **101**, 32 (1993).
- [25] F. Diedrich, E. Peik, J.M. Chen, W. Quint, and H. Walther, *Phys. Rev. Lett.* **59**, 2931 (1987).
- [26] D.J. Wineland, J.C. Bergquist, W.M. Itano, J.J. Bollinger, and C.H. Manney, *Phys. Rev. Lett.* **59**, 2935 (1987).
- [27] R.G. DeVoe, J. Hoffnagle, and R.G. Brewer, *Phys. Rev. A* **39**, 4362 (1989).
- [28] R. Blümel, C. Kappler, W. Quint, and H. Walther, *Phys. Rev. A* **40**, 808 (1989); **46**, 8034(E) (1992).
- [29] For the optical excitation this condition is already fulfilled if there is an integer  $m$  such that  $|\Omega - m\omega| < \Gamma$ . Experimentally, an exact integer ratio between the frequencies will usually be avoided because it can lead to parametric excitation of the secular motion through the trapping field [see R. Alheit, C. Hennig, R. Morgenstern, F. Vedel, and G. Werth, *Appl. Phys. B: Lasers Opt.* **61**, 277 (1995)].
- [30] T. Sauter, H. Gilhaus, W. Neuhauser, R. Blatt, and P. Toschek, *Europhys. Lett.* **7**, 317 (1988).
- [31] E. Peik, G. Hollemann, and H. Walther, *Phys. Scr.* **T59**, 403 (1995).
- [32] E.L. Pollock and J.P. Hansen, *Phys. Rev. A* **8**, 3110 (1973).
- [33] I. Waki, S. Kassner, G. Birkel, and H. Walther, *Phys. Rev. Lett.* **68**, 2007 (1992).
- [34] M.G. Raizen, J.M. Gilligan, J.C. Bergquist, W.M. Itano, and D.J. Wineland, *Phys. Rev. A* **45**, 6493 (1992).
- [35] B.E. King, C.S. Wood, C.J. Myatt, Q.A. Turchette, D. Leibfried, W.M. Itano, C. Monroe, and D.J. Wineland, *Phys. Rev. Lett.* **81**, 1525 (1998).
- [36] E. Peik, G. Hollemann, C. Schrama, and H. Walther, *Laser Phys.* **4**, 376 (1994).
- [37] R. Blümel, J.M. Chen, E. Peik, W. Quint, W. Schleich, Y.R. Shen, and H. Walther, *Nature (London)* **334**, 309 (1988).